

# First-principles pseudopotential calculations of the elastic properties of diamond, Si, and Ge

A. Fukumoto

*Toyota Central Research & Development Laboratories, Inc., 41-1 Aza Yokomichi, Oaza Nagakute,  
Nagakute-cho, Aichi-gun, Aichi-ken 480-11, Japan*

(Received 13 March 1990; revised manuscript received 22 May 1990)

The reason why diamond has much different elastic properties, in particular a much smaller Poisson ratio, compared with Si and Ge is investigated using an *ab initio* pseudopotential method within the local-density-functional formalism. Besides the Poisson ratios, the equilibrium lattice constants, bulk moduli, elastic constants, and internal strain parameters are calculated. Good agreement with experiment is obtained. In order to eliminate the effects of the equilibrium-volume difference among these crystals, the reduced-second-volume derivatives are introduced into the individual energy terms. It is clearly shown that the kinetic energy and the ion-electron interaction energy play important roles in the response to homogeneous volume change and to distortions, respectively. The charge-density distributions display much different responses to strains between diamond and the others.

## I. INTRODUCTION

There have been many successful first-principles calculations on the ground-state properties of a wide range of solids. Most of them are based on the local-density-functional theory,<sup>1</sup> where a single-particle Schrödinger equation is solved self-consistently. Various techniques<sup>2-5</sup> have been used for applying this theory according to the characteristics of the materials. One important technique is the norm-conserving pseudopotential approach,<sup>6</sup> which has produced much improvement in the reliability of the calculations for valence states. We have applied these methods in order to investigate the elastic properties of group-IV covalent crystals. A detailed investigation of these elastic properties is very important since these materials are widely used in the solid-state devices.

The elastic properties of diamond are different in many respects from those of Si and Ge, although these three materials have the same crystal structure. Many papers<sup>7-18</sup> have been published in which the ground-state properties of C, Si, and Ge were investigated with the first-principles pseudopotential calculations. However, there have been no studies that deal with the similarity and/or discrepancy of the Poisson ratios among these three materials. Si and Ge have almost the same values of the Poisson ratios, while diamond has much smaller values. In this paper, the equilibrium lattice constants, bulk moduli, elastic constants, internal strain parameters, and Poisson ratios are calculated, and several distinctive features between diamond and the others are discussed. The most obvious and elementary discrepancy among them is the equilibrium volume. We introduce a reduced scale for volume in order to eliminate the effects of the volume difference. The purpose of this study is to clarify the causes of the discrepancy and/or similarity of the elastic properties among the three materials with the reduced scale for volume.

This paper is organized as follows. In Sec. II, the cal-

culational procedure is described. Section III presents the results, and the discussions of the results are given in Sec. IV. Section V summarizes the present work.

## II. METHOD

The calculational procedures are based upon the Hohenberg-Kohn-Sham local-density-functional formalism.<sup>1</sup> We use hartree atomic units in this paper. The ground-state total energy of a many-electron system can be written in the form

$$E_{\text{tot}} = T_s[\rho(\mathbf{r})] + \int V_{\text{ext}}(\mathbf{r})\rho(\mathbf{r})d\mathbf{r} + \frac{1}{2} \iint \frac{\rho(\mathbf{r})\rho(\mathbf{r}')}{|\mathbf{r}-\mathbf{r}'|} d\mathbf{r}d\mathbf{r}' + E_{\text{xc}}[\rho], \quad (1)$$

where  $\rho(\mathbf{r})$  is the electronic charge density,  $T_s$  is the kinetic energy of a noninteracting electron gas of density  $\rho(\mathbf{r})$ , and  $V_{\text{ext}}$  is an external potential which usually represents the potential due to the nuclei.  $E_{\text{xc}}$  is the exchange-correlation energy functional, which is given in the local-density-functional approximation as

$$E_{\text{xc}}[\rho(\mathbf{r})] = \int \epsilon_{\text{xc}}(\rho(\mathbf{r}))\rho(\mathbf{r})d\mathbf{r}, \quad (2)$$

where  $\epsilon_{\text{xc}}(\rho)$  is the exchange-correlation energy per electron in a homogeneous electron gas of density  $\rho$ .

The charge density  $\rho$  is determined self-consistently by solving the Kohn-Sham equation

$$[-\frac{1}{2}\Delta + V_{\text{ext}}(\mathbf{r}) + V_H(\mathbf{r}) + V_{\text{xc}}(\rho)]\psi_i(\mathbf{r}) = \epsilon_i\psi_i(\mathbf{r}), \quad (3)$$

with

$$\rho(\mathbf{r}) = \sum_i n_i |\psi_i(\mathbf{r})|^2, \quad (4)$$

where  $n_i$ ,  $\epsilon_i$ , and  $\psi_i$  are the occupation number, eigenvalue, and the wave function of the one-electron state  $i$ , respectively.  $V_H(\mathbf{r})$  is the electronic Hartree potential,

$$V_H(\mathbf{r}) = \int \frac{\rho(\mathbf{r}')}{|\mathbf{r}-\mathbf{r}'|} d\mathbf{r}', \quad (5)$$

and  $V_{xc}(\rho)$  is the exchange-correlation potential,

$$V_{xc}(\rho) = \frac{d(\rho\epsilon_{xc})}{d\rho}. \quad (6)$$

There are several approaches for solving these equations.<sup>2-5</sup> Among them, the pseudopotential approach<sup>6</sup> seems to be most suitable for studying the properties of semiconductors. In this approach,  $V_{ext}$  is replaced by an ionic pseudopotential. The total energy can be written by

$$E_{tot} = E_k + E_{ce} + E_{ee} + E_{xc} + E_{cc}. \quad (7)$$

The individual contributions can be interpreted as the electronic kinetic energy, the core(ion)-electron interaction energy, the electron-electron Coulomb energy, the exchange-correlation energy, and the core-core Coulomb energy (the Ewald energy), respectively. The term "electrons" refers to valence electrons only. The ionic pseudopotentials are represented by the norm-conserving nonlocal pseudopotentials, which are shown in Fig. 1. These are generated numerically through the Hamann-Schlüter-Chiang method.<sup>6</sup> The  $p$  potential of C is much deeper than that of Si and Ge since the carbon atom does not have  $p$  electrons in the core. The  $d$  potential of Ge is more repulsive than that of C and Si for a similar reason. These potentials are fitted to analytic functions according to the method of Bachelet, Hamann, and Schlüter,<sup>19</sup> however we use five Gaussians for fitting the nonlocal (angular-momentum-dependent) part. The Wigner interpolation formula<sup>20</sup> for the exchange-correlation energy is used both in the atomic and crystalline calculations.

A plane-wave basis set is used to represent the valence wave functions. The total-energy calculations are performed with the momentum-space formalism.<sup>21</sup> There are two procedures to introduce a cutoff on the reciprocal-lattice vectors to be included in the basis set. The procedure with a fixed cutoff energy of the plane-wave kinetic energy leads to a varying number of plane waves when a crystal structure is changed. Another one with a fixed number of plane waves even when the structure is varied leads to much smoother total-energy curves. We employ the latter procedure since it is convenient for calculating the smooth change of the total energy due to strains. The number of plane waves is 537, 283, and 339 for diamond, Si, and Ge, respectively.

The Brillouin-zone  $\mathbf{k}$  integration is performed by the special-points scheme of Chadi and Cohen<sup>22</sup> and Monkhorst and Pack.<sup>23</sup> The number of  $\mathbf{k}$  points are 10 for the cubic lattice and 20 and 30 for the lattice with strains along [001] and [111], respectively.

We calculate the equilibrium lattice constants ( $a$ ), bulk moduli ( $B$ ), elastic constants ( $C_{ij}$ 's), internal strain parameters ( $\zeta$ ), and Poisson ratios ( $\mu_{ijk}$ 's) of diamond, Si, and Ge. The equilibrium lattice constants and bulk moduli are determined from quadratic fits to the total-energy values which are calculated for different lattice constants ranging from  $-1\%$  to  $+1\%$  of the experimental values.

Although it is convenient to apply the "stress

theorem" proposed by Nielsen and Martin<sup>24</sup> in order to calculate the elastic constants, we obtain  $C_{ij}$ 's with a standard fitting procedure in order to unify the method for obtaining the Poisson ratio, which will be discussed later. The elastic constants  $C_{11}$  and  $C_{12}$  are determined

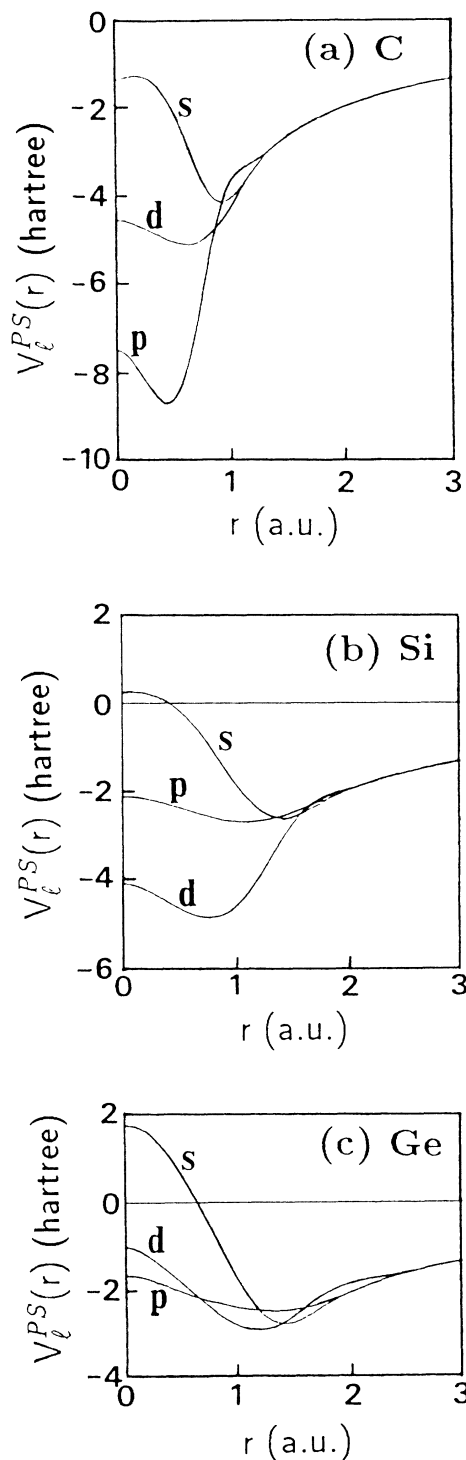


FIG. 1. Norm-conserving pseudopotentials of (a) C, (b) Si, and (c) Ge. The potentials are generated using the method described in Refs. 6 and 19.

by  $B [(C_{11}+2C_{12})/3]$ , and the shear modulus  $C_{11}-C_{12}$ . In order to calculate the shear modulus, we introduce a homogeneous tetragonal distortion, in which the length scales of the three cubic directions are changed by  $1+\epsilon$ ,  $1+\epsilon$ , and  $(1+\epsilon)^{-2}$ , respectively, while the atomic volume is kept constant. The total energy is related to  $C_{11}-C_{12}$  by

$$E_{\text{tot}} = E_0 + 3V_0(C_{11}-C_{12})\epsilon^2 + O(\epsilon^3), \quad (8)$$

where  $V$  is the atomic volume and the subscript 0 indicates its equilibrium value. Total energies are calculated with the value of  $\epsilon$  varying from  $-0.01$  to  $+0.01$ . The calculation of  $C_{44}$  is more complicated than that of  $C_{11}$  and  $C_{12}$ . A strain  $\epsilon_{yz} = \epsilon_{zx} = \epsilon_{xy} = \epsilon_4/2$  (the Voigt notation) along the  $[111]$  direction of a diamond lattice makes the  $[111]$  atomic bond inequivalent to the other  $[\bar{1}\bar{1}1]$ ,  $[\bar{1}\bar{1}\bar{1}]$ , and  $[\bar{1}\bar{1}\bar{1}]$  bonds. The atomic positions in the unit cell are no longer completely determined by symmetry. Kleinman<sup>25</sup> defined an internal strain parameter  $\zeta$  such that the value  $\zeta=0$  corresponds to a perfect strain of atomic positions and  $\zeta=1$  corresponds to a rigid bond length. In order to obtain  $\zeta$ , the total-energy values are calculated for several values of  $\epsilon_4$  and varying  $\zeta$ .  $\zeta$  is determined so that the total energy attains its minimum value for a fixed  $\epsilon_4$ . Thus,  $\zeta$  can be obtained as the function of  $\epsilon_4$ .  $C_{44}$  is determined from quadratic fits to the total-energy values per atom.  $\epsilon_4$  is varied from  $-0.01$  to  $+0.01$ .

Although the Poisson ratios can be evaluated with the theory of elasticity as

$$\mu_{001} = \frac{C_{12}}{C_{11} + C_{12}}, \quad (9)$$

$$\mu_{111} = \frac{1}{2} \frac{C_{11} + 2C_{12} - 2C_{44}}{C_{11} + 2C_{12} + C_{44}}, \quad (10)$$

we also calculate  $\mu_{ijk}$ 's another way. We introduce strains of 1% elongation along  $[ijk]$  directions. The total energy is minimized with varying the length perpendicular to  $[ijk]$ . For an elongation along  $[001]$ , the length of the three cubic directions are changed to  $b$ ,  $b$ , and  $c$ , where  $c = 1.01a$  ( $a$  is the equilibrium lattice constant).  $b$  is determined so that the total energy has its minimum value with a fixed  $c$  value.  $\mu_{001}$  can be obtained as  $(a-b)/(c-a)$ . For an elongation along  $[111]$ , the unit vectors are altered to  $(d, \delta, \delta)$ , and its cyclic permutations, satisfying a condition  $d + 2\delta = 1.01a$ .  $\delta/d$  is determined by minimizing the total energy similarly. For an elongation along  $[110]$ , we cannot define the Poisson ratio  $\mu_{110}$  in the ordinary way since the  $[\bar{1}10]$  direction and the  $[001]$  direction are geometrically inequivalent. In this case, we have to define two "extended" Poisson ratios, say  $\mu_{110}^{\bar{1}10}$  and  $\mu_{110}^{001}$ . Therefore, we do not calculate  $\mu_{110}$  with the energy-minimization approach mentioned above. These values obtained with the theory of elasticity can be written as follows:

$$\mu_{110}^{\bar{1}10} = \frac{(1-p)(1+2p)-2q}{(1-p)(1+2p)+2q}, \quad (11)$$

$$\mu_{110}^{001} = \frac{4pq}{(1-p)(1+2p)+2q}, \quad (12)$$

where  $p = C_{12}/C_{11}$  and  $q = C_{44}/C_{11}$ .

### III. RESULTS

The calculated lattice constants ( $a$ ), bulk moduli ( $B$ ), elastic constants ( $C_{ij}$ 's), internal strain parameters ( $\zeta$ ) and their rate of change, and Poisson ratios ( $\mu_{ijk}$ 's) are compared with experiments in Table I. The agreement is very good. The Poisson ratios shown in the upper row of

TABLE I. Lattice constants  $a$ , bulk moduli  $B$ , elastic constants  $C_{ij}$ , internal strain parameters  $\zeta$ , rates of change of  $\zeta$ , and Poisson ratios  $\mu_{ijk}$  of diamond, Si, and Ge. The values of  $\mu_{ijk}$ 's in the upper row are obtained theoretically with  $C_{ij}$ 's, and in the lower row are obtained by the total-energy-minimization approach with a fixed (1%) elongation along  $[ijk]$ .

	C		Si		Ge	
	Calc.	Expt.	Calc.	Expt.	Calc.	Expt.
$a$ (Å)	3.556	3.567 <sup>a</sup>	5.419	5.429 <sup>a</sup>	5.620	5.652 <sup>a</sup>
$B$ (Mbar)	4.64	4.42 <sup>b</sup>	0.979	0.992 <sup>d</sup>	0.778	0.768 <sup>d</sup>
$C_{11}$ (Mbar)	10.97	10.81 <sup>c</sup>	1.663	1.675 <sup>d</sup>	1.377	1.315 <sup>d</sup>
$C_{12}$ (Mbar)	1.48	1.25 <sup>c</sup>	0.633	0.650 <sup>d</sup>	0.482	0.494 <sup>d</sup>
$C_{44}$ (Mbar)	5.82	5.79 <sup>c</sup>	0.793	0.801 <sup>d</sup>	0.717	0.684 <sup>d</sup>
$\zeta$	0.12		0.53	0.54 <sup>e</sup>	0.51	0.54 <sup>e</sup>
$\partial\zeta/\partial\epsilon_4$	-2.0		-1.2		-1.4	
$\mu_{001}$	0.119	0.104	0.276	0.280	0.259	0.273
	0.114		0.271		0.262	
$\mu_{111}$	0.058	0.045	0.180	0.182	0.148	0.157
	0.052		0.180		0.161	
$\mu_{110}^{\bar{1}10}$	0.017	0.008	0.067	0.064	0.030	0.025
$\mu_{110}^{001}$	0.133	0.115	0.355	0.363	0.340	0.366

<sup>a</sup>J. Donohue, *The Structure of Elements* (Wiley, New York, 1974).

<sup>b</sup>H. J. McSkimin and P. Andreatch, *J. Appl. Phys.* **43**, 985 (1972).

<sup>c</sup>H. J. McSkimin and P. Andreatch, *J. Appl. Phys.* **43**, 2944 (1972).

<sup>d</sup>H. J. McSkimin, *J. Appl. Phys.* **24**, 988 (1953); H. J. McSkimin and P. Andreatch, *ibid.* **35**, 3312 (1964).

<sup>e</sup>C. S. G. Cousins, L. Gerward, J. Staun Olsen, B. Selsmark, and B. J. Sheldon, *J. Phys. C* **20**, 29 (1987).

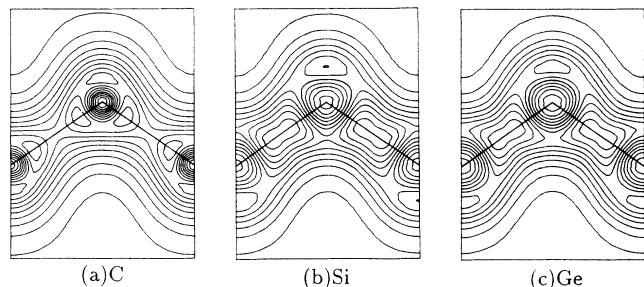


FIG. 2. Contour plots of the valence charge density in the (110) plane of (a) C, (b) Si, and (c) Ge. The bond-charge maxima are  $3.0 \times 10^{-1}$ ,  $8.4 \times 10^{-2}$ , and  $7.4 \times 10^{-2}$  in atomic units, respectively. The bonding directions are illustrated by the straight lines. The contours are subdividing between the maximum and minimum values into 10 steps. The intervals are  $2.9 \times 10^{-2}$  for (a),  $8.1 \times 10^{-3}$  for (b), and  $7.1 \times 10^{-3}$  for (c).

Table I are obtained by Eqs. (9)–(12) with the elastic constants, and those in the lower row are obtained by the total-energy-minimization approach. Both of them are almost the same.

Contour plots of the valence charge-density distributions in the (110) plane are shown in Fig. 2. Similar to previous studies,<sup>7,8,13,17</sup> very pronounced two-peak structure of the bond-charge density can be seen for diamond. The major contribution to this feature is from the *p*-like valence bonds. The C atom has a deep *p* potential near the nucleus as shown in Fig. 1. This is due to the lack of core *p* states. For Si and Ge, the charge contours exhibit an elongated form in the bonding charge. Although Ge has a repulsive *d* potential, it is not effective to the valence charge-density distribution since Ge has no *d* valence electrons. Figure 3 shows the changes of the charge densities in the (110) plane due to the homogeneous volume change (hydrostatic pressure). The functions plotted are the density at the equilibrium volume minus the density at the lattice constant increased by 1%, after

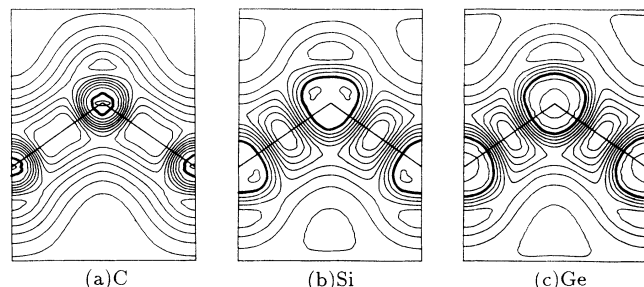


FIG. 3. The changes of the valence charge density in the (110) plane due to the homogeneous volume change. The functions plotted are the density at the equilibrium volume minus the density at the lattice constant increased by 1%, after both of them are projected on the same plane. The thick contour denotes zero. The contour steps are defined similar to Fig. 2. The intervals are  $6.9 \times 10^{-4}$  for (a),  $2.8 \times 10^{-4}$  for (b), and  $2.6 \times 10^{-4}$  for (c) in atomic units.

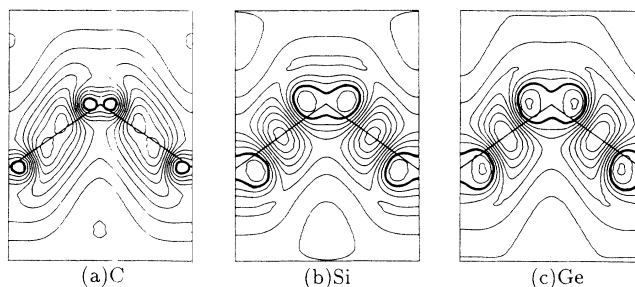


FIG. 4. The changes of the valence charge density in the [110]-[001] plane due to the compression perpendicular to [001]. The thick contour denotes zero. The intervals are  $5.6 \times 10^{-4}$  for (a),  $2.5 \times 10^{-4}$  for (b), and  $2.4 \times 10^{-4}$  for (c) in atomic units.

these two densities are projected on the same plane. In diamond, the most rapidly increasing parts exist along the bond, which is a common feature with the deformation density (defined as the valence charge density minus the density of overlapping free pseudoatoms) in Fig. 1 of Ref. 18. In Si and Ge, the most rapidly increasing parts are spread away from the bond, which is not very similar to the deformation density in Fig. 1 of Ref. 16 (almost spherical). The density changes in the [110]-[001] plane due to strains are shown in Figs. 4 and 5. The functions plotted in Fig. 4 are the density of the stable structure compared with  $\mu_{001}$  (with 1% elongation along [001]) minus the density at the lattice constant increased by 1%, after the similar projection. The two-peak structure can be clearly seen again in diamond, however the distance between the two-peak points is rather short. The difference from Fig. 3 is smaller in Si and Ge. For a strain along [111], it is not meaningful to subtract one density from another as was done above because of the internal strain. In this case, the atomic positions do not coincide with each other after the projection. However, we can obtain some information about the response of the densities to the distortion. Similar plots for an elongation along [111] are shown in Fig. 5. The functions plotted are the density of the stable structure compared to  $\mu_{111}$

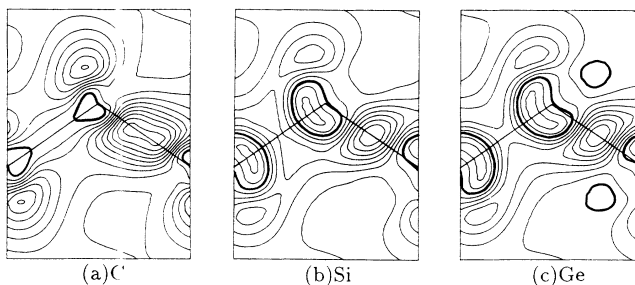


FIG. 5. The changes of the valence charge density in the [110]-[001] plane due to the compression perpendicular to [111]. The thick contour denotes zero. The left-hand bond is oriented along [111] and the right-hand bond is oriented along  $[1\bar{1}\bar{1}]$ . The intervals are  $6.9 \times 10^{-4}$  for (a),  $2.7 \times 10^{-4}$  for (b), and  $3.0 \times 10^{-4}$  for (c) in atomic units.

(with 1% elongation along [111]) minus the density at the lattice constant increased by 1%, after the projection. Two distributions are projected so that the bond centers coincide with each other. In Fig. 5, the left-hand bond is oriented along [111] and the right-hand bond is oriented along  $[1\bar{1}\bar{1}]$ . The bond charges increase more in the right-hand bond in every material. In the left-hand bond, the bond charge hardly increases in diamond.

The dependence of the individual energy terms on volume or on distortions can be considered to play an important role in the elastic properties of solids. The first- and second-volume derivatives of the individual energy terms of diamond, Si, and Ge are listed in Table II. The volume derivatives in the elongated lattices are calculated with the fixed (1%) elongation along  $[ijk]$  and varying the lengths perpendicular to  $[ijk]$ . The first-volume derivatives are not very varied among the three kinds of strains, while the second derivatives depend fairly strongly on the kinds of strains. The difference of the equilibrium volume among the three materials has much influence on the absolute values of the volume derivatives shown in Table II. The kinetic energy scales as  $V^{-2/3}$ , and the other terms scale as  $V^{-1/3}$ , approximately. In order to eliminate the effect of the volume difference, we change the length scale according to the equilibrium volume of each material. The reduced-second-volume derivatives of the individual energy terms can be defined as follows:

Kinetic energy ,

$$\frac{m}{\hbar^2} V_0^{8/3} \frac{\partial^2 E_k}{\partial V^2} ; \quad (13)$$

other terms ,

$$\frac{1}{e^2} V_0^{7/3} \frac{\partial^2 E_{\text{stat}}}{\partial V^2} ; \quad (14)$$

where the subscript stat represents one of  $ce$ ,  $ee$ ,  $xc$ , or  $cc$ . The results are shown in Table III. With this alteration of the length scale, the reduced derivatives of  $E_k$ ,  $E_{ee}$ , and  $E_{xc}$  depend, approximately, only on the shape of the charge densities. The reduced derivative of  $E_{ce}$  depends on the density and the (pseudo)potentials.  $E_{cc}$  is a constant term independent of the density. Therefore,  $E_{cc}$ 's have the same values among the three materials except for the case elongated along [111]. The discrepancy in  $E_{cc}$  of diamond for an elongation along [111] is due to the difference of the internal strain parameters between diamond and the others. Si and Ge have almost the same reduced derivatives in every term in every structure since both have the similar pseudopotentials (except for  $d$ ) and similar charge-density distributions.  $E_{ce}$  and  $E_{ee}$  are very sensitive to the different kinds of strains. Diamond has different values, particularly in these two terms ( $E_{ce}$  and  $E_{ee}$ ), compared to Si and Ge. This is due to the deep  $p$  potential and the distinctive two-peak structure in the bond charge of C. Although much-higher-order components are used in the basis functions for diamond, it has no influence on the reduced-second-volume derivative of  $E_k$ . Figure 3(a) is similar to Figs. 2(b) and 2(c). This means that higher-order components have few effects on the changes of charge density.

#### IV. DISCUSSION

We can confirm with Table I that diamond has very distinctive elastic features compared to Si and Ge. Diamond has a much smaller equilibrium lattice constant, a much larger bulk modulus and elastic constants, relatively small  $C_{12}$ , a much smaller internal strain parameter, and a much smaller Poisson ratio. We discuss the reason for these features with the response of the individual en-

TABLE II. First- and second-volume derivatives of the individual energy terms in units of  $\text{eV}/\text{\AA}^3$  and  $\text{eV}/\text{\AA}^6$ , respectively. The values indicated by [001] and [111] are calculated with a fixed length (1% elongation) along  $[ijk]$  and varying the lengths perpendicular to  $[ijk]$ .

		First derivative			Second derivative		
		C	Si	Ge	C	Si	Ge
Cubic	$E_k$	-8.24	-0.893	-0.665	1.3	0.046	0.034
	$E_{ce}$	-5.22	-1.66	-1.55	0.51	0.052	0.040
	$E_{ee}$	1.17	0.280	0.272	-0.05	-0.004	-0.003
	$E_{xc}$	1.94	0.356	0.296	-0.26	-0.013	-0.010
	$E_{cc}$	10.4	1.92	1.65	-1.2	-0.064	-0.049
[001]	$E_k$	-8.11	-0.881	-0.655	1.2	0.042	0.031
	$E_{ce}$	-5.30	-1.67	-1.56	0.99	0.074	0.057
	$E_{ee}$	1.20	0.287	0.278	-0.21	-0.012	-0.009
	$E_{xc}$	1.91	0.351	0.292	-0.22	-0.011	-0.009
	$E_{cc}$	10.3	1.92	1.65	-1.4	-0.075	-0.057
[111]	$E_k$	-8.15	-0.880	-0.661	1.3	0.044	0.033
	$E_{ce}$	-5.05	-1.65	-1.55	-0.10	0.055	0.044
	$E_{ee}$	1.12	0.278	0.270	0.16	-0.003	-0.003
	$E_{xc}$	1.92	0.351	0.294	-0.25	-0.012	-0.009
	$E_{cc}$	10.2	1.91	1.64	-0.78	-0.066	-0.051

TABLE III. Reduced-second-volume derivatives of the individual energy terms defined by Eqs. (13) and (14).

		C	Si	Ge
Cubic	$E_k$	17	17	17
	$E_{ce}$	2.0	3.8	3.9
	$E_{ee}$	-0.20	-0.33	-0.32
	$E_{xc}$	-1.0	-1.0	-1.0
	$E_{cc}$	-4.8	-4.8	-4.8
[001]	$E_k$	16	16	16
	$E_{ce}$	3.9	5.6	5.6
	$E_{ee}$	-0.81	-0.92	-0.92
	$E_{xc}$	-0.88	-0.84	-0.86
	$E_{cc}$	-5.6	-5.6	-5.6
[111]	$E_k$	18	17	17
	$E_{ce}$	-0.40	4.2	4.3
	$E_{ee}$	0.66	-0.19	-0.26
	$E_{xc}$	-0.98	-0.89	-0.90
	$E_{cc}$	-3.1	-5.0	-5.0

ergy terms and the charge densities to strains.

The lattice constant of diamond is much less than that of Si and Ge. This is obviously due to the deep pseudopotentials of C, in particular for the  $p$  state. Whereas, we can find another interesting discrepancy between diamond and the others by changing the length scale. We define the atomic radius  $r_a$  as the point where the charge-density value of an isolated atom with  $sp^3$  valence configuration is equal to the average-charge-density value in the equilibrium volume, that is,  $4/V_0$ . The half bondlengths,  $r_a$ 's, and their ratios are shown in Table IV. Si and Ge have the same ratio, while diamond has a larger value. Diamond has a "long" bondlength as compared with the atomic radius. This result suggests that the contraction of the volume by condensation occurs more in Si and Ge than in diamond. This is consistent with the fact that the change of the charge density of diamond caused by the homogeneous-volume change shown in Fig. 3(a) is similar to the deformation density of diamond in Ref. 18, while that of Si in Fig. 3(b) is not very similar to the deformation density in Ref. 16. Diamond has much larger first- and second-volume derivatives in the kinetic energy than in the other terms compared to Si and Ge because of the small lattice constant.  $E_k$  has a stronger dependence on the volume than the other terms. It scales as the volume to the power of  $-\frac{2}{3}$ , while the other terms scale as to the power of  $-\frac{1}{3}$ . The rapidly increasing kinetic en-

TABLE IV. Half bondlengths, atomic radii ( $r_a$ ) in units of Å, and their ratios. For the definition of  $r_a$ , see text.

	Half bondlength	$r_a$	Ratio
C	0.77	0.87	0.89
Si	1.17	1.41	0.83
Ge	1.22	1.47	0.83

ergy with the compression keeps the bondlength "long" in diamond.

The bulk modulus of diamond is much larger than that of Si and Ge. However, with the homogeneous-volume change, diamond has a smaller value of the reduced-second-volume derivative of  $E_{ce}$  than Si and Ge. This is due to the difference of the pseudopotentials. The other energy terms have roughly the same reduced-second-volume derivatives among the three materials. These are consistent with the results obtained by Martin<sup>26</sup> using the valence-force-field model.<sup>27</sup> He defined the reduced bulk modulus  $B^*$  as

$$B^* = (C_{11} + 2C_{12})/3C_0, \quad (15)$$

$$C_0 = e^2/r^4,$$

where  $r$  is the equilibrium bondlength.  $B^*$  of diamond, Si, and Ge are 1.091, 1.298, and 1.173, respectively (see Table III of Ref. 26). His result that diamond has the least reduced bulk modulus can be considered as having close relationship to the fact that diamond has a small reduced-second-volume derivative of  $E_{ce}$  in this study. The large bulk modulus of diamond is only due to the small equilibrium volume, in which the second-volume derivative of the kinetic energy is very large. It is important again that  $E_k$  has a stronger dependence on the volume than the other terms. The contribution of  $E_k$  to the total energy can be identified as being responsible for the elastic properties related to the homogeneous-volume change.

The elastic constants of diamond are larger than those of Si and Ge. This is due to the difference of the equilibrium volume discussed above. Another feature is that diamond has a relatively small  $C_{12}$ . Diamond also has a much smaller internal strain parameter. Both of these two properties have relevance to the bond bending. According to Keating,<sup>28,29</sup>  $C_{ij}$ 's and  $\zeta$  can be written as

$$C_{11} = \frac{\alpha + 3\beta}{4a}, \quad (16)$$

$$C_{12} = \frac{\alpha - \beta}{4a}, \quad (17)$$

$$C_{44} = \frac{\alpha\beta}{a(\alpha + \beta)}, \quad (18)$$

$$\zeta = \frac{\alpha - \beta}{\alpha + \beta}, \quad (19)$$

where  $\alpha$  is the bond-stretching force constant and  $\beta$  is the bond-bending force constant. Small values of  $C_{12}$  and  $\zeta$  mean a large  $\beta$ . The shear modulus  $C_{11} - C_{12}$  is proportional to  $\beta$ . In order to investigate the contributions to the bond-bending force constant, the second derivatives of the individual energy terms with respect to  $\epsilon$  used in Eq. (8) are calculated and listed in Table V. The reduced scale is not used since the volumes are kept constant here. The large second derivative in the total energy of diamond means that it has strong tendency to keep the regular tetrahedral configuration. A major contribution of the large second derivative comes from  $E_{ce}$ , which depends on the pseudopotentials. The deep  $p$  pseudopotential

TABLE V. Second derivatives of the individual energy terms with respect to the tetragonal distortion  $\epsilon$  [see Eq. (8)] (in hartrees).

	C	Si	Ge
$E_k$	-3.6	-1.8	-1.5
$E_{ce}$	20	13	12
$E_{ee}$	-6.4	-4.2	-4.0
$E_{xc}$	1.6	1.1	1.1
$E_{cc}$	-8.0	-5.6	-5.4
$E_{tot}$	4.4	1.5	1.3

tial of diamond attracts valence  $p$  electrons close to the nucleus. The valence  $s$  electrons also exist near the nucleus. Both have almost the same radii for maxima in radial wave functions. The valence  $d$  electrons, which have a larger principal quantum number by 1, are extended from the nucleus in the C atom. On the other hand, Si and Ge have shallow pseudopotentials and have different radii for maxima in  $s$  and  $p$  radial wave functions. They have closer radii for maxima in  $d$  radial wave function compared with C. These features make diamond more stable with the  $sp^3$  bonding than Si and Ge. A similar result can be also derived from considering the energy eigenvalues. A bending distortion introduces a  $d$  (or still higher angular-momentum) symmetry into the  $sp^3$  hybridization. The energy eigenvalues of the  $p$  state of the isolated atom with  $s^2p^{0.5}d^{0.5}$  configuration are  $-0.78$ ,  $-0.47$ , and  $-0.47$  hartrees for C, Si, and Ge, respectively. Those of the  $d$  state are  $-0.14$ ,  $-0.17$ , and  $-0.15$  hartrees, respectively. The  $d$  orbital existing at relatively high energy in the C atom causes a rapid increase in  $E_{ce}$  with a bond bending in diamond. We can conclude that the behavior of  $E_{ce}$  leads to the relatively small  $C_{12}$  and small  $\zeta$  in diamond.

Diamond has a much smaller Poisson ratio than Si and Ge. The influence of the different  $\mu_{001}$  among these three materials can be seen clearly in the contour plots in Fig. 4. These figures show the response of the charge densities to a compression perpendicular to [001]. Si and Ge show a similar response, and they have almost the same  $\mu_{001}$ . In diamond, the two-peak structure can again be seen; it is hardly seen in the response to the homogeneous-volume change shown in Fig. 3(a). Moreover, the most rapidly increasing points are not on the bond. They are located so that the maximum points of the bond charge are not brought closer to the neighboring maximum points by this kind of compression in order to lower the hartree energy. This is due to the two-peak structure of the bond charge. This character can be considered to have some contributions in making the bond-bending-force constant large in diamond. In the volume derivatives of the individual energy terms, the most remarkable difference between the lattice elongated along [001] and the cubic lattice occurs in  $E_{ce}$  of diamond. The ratios of the second derivative of  $E_{ce}$  between the lattice elongated along [001] and the cubic lattice are about 2.0 for diamond and about 1.5 for Si and Ge. This means that, in real scale,  $E_{ce}$  increases more rapidly in diamond than Si and Ge with the compression perpendicular to [001].

The energy terms, except for  $E_{ce}$ , have almost the same tendency between cubic and [001] in the three materials, as can be seen easily with the reduced scale in Table III. The small  $\mu_{001}$  in diamond is mainly due to the fact that diamond has a different response of the ion-electron interaction energy, compared to Si and Ge, to a compression perpendicular to [001]. This compression is accompanied by the bond bending. As has already been shown in Table V,  $E_{ce}$  has the largest effect on the response to the bond bending. The stability of  $sp^3$  hybridization due to the deep  $p$  pseudopotential in C makes  $\mu_{001}$  small. To put it in other words, the large bond-bending force constant in diamond makes  $C_{12}$  relatively small and leads to a small Poisson ratio  $\mu_{001}$  through the relation of Eq. (9).

For the compression perpendicular to [111], the response of the charge densities shows a considerable discrepancy between diamond and the others, as shown in Fig. 5. Diamond strongly favors the  $sp^3$  hybridization and it makes  $\zeta$  small. The small  $\zeta$  (or the large bond-bending force constants) of diamond makes the [111] bondlength (and other equivalents) still shorter than the [111] bondlength compared with Si and Ge. In order to compensate for the increase in nuclear Coulomb repulsion, bond charge increases much in the bond along [111] (and its equivalents). It hardly increases in the [111] bond. This feature is weaker in Si and Ge because the  $\zeta$ 's are larger. The most rapidly increasing points of the charge density are not on the bond in diamond, for a similar reason to the case of the compression perpendicular to [001]. Considering the individual energy terms, many features can be found in Tables II and III. The difference of the second-volume derivatives between the lattice elongated along [111] and the cubic lattice is much different from the difference between the lattice elongated along [001] and the cubic lattice in diamond. The first derivatives of  $E_{ce}$  and  $E_{ee}$  vary reversely. The signs of the second derivatives of  $E_{ce}$  and  $E_{ee}$  are changed. Diamond has the least absolute value of the second-volume derivative of  $E_{cc}$  in the compression perpendicular to [111], while Si and Ge do not. Si and Ge have almost the same second derivatives in the reduced scale, except for a small difference in  $E_{ee}$ . The effect of the difference of the bond-bending force constant does not appear directly in  $E_{ce}$  as in the case of the compression perpendicular to [001]. These complicated features are due to the internal strain. Diamond has about one-fourth the value of  $\zeta$  compared with Si and Ge, since the  $sp^3$  hybridization is more stable in C. Consequently, the second-volume derivatives of  $E_{cc}$  and  $E_{ee}$  increase (negatively decrease for  $E_{cc}$ ) greatly in diamond. They make major contributions to the increase of the total energy in diamond by a compression perpendicular to [111] and lead to a small  $\mu_{111}$  in diamond.

We have made it clear that the cause of the small  $C_{12}$  (relative value),  $\zeta$ , and  $\mu_{001}$  of diamond can be attributed to the stability of  $sp^3$  hybridization, to which  $E_{ce}$  plays a major role. The values of  $\mu_{111}$  are affected by  $E_{ce}$  indirectly through  $\zeta$ . The volume derivatives of  $E_{ce}$  are very sensitive to the various kinds of strains and have much different values between diamond and the others in

the reduced scale. The contribution of  $E_{ce}$  to the total energy can be identified as being responsible for the different elastic properties related to distortions between diamond and the others.

## V. SUMMARY

We have investigated the elastic properties of diamond, Si, and Ge. The calculated lattice constants, bulk moduli, elastic constants, internal strain parameters, and Poisson ratios agree well with experiments. Diamond has many different features in these properties compared with Si and Ge. This reason has been investigated by eliminating the effect of the equilibrium-volume difference. In the reduced scale, the lattice constant of diamond is large. The large bulk modulus of diamond is due to its small equilibrium volume, where the kinetic energy has very large second-volume derivative. The difference of the elastic constants, internal strain parameter, and Poisson ratio  $\mu_{001}$  are due to the different response to distortions of  $E_{ce}$ , which has the most distinctive values of the reduced-second-volume derivatives between diamond and the others. The response to a strain applied along [111] is more complicated than that along [001] since the internal

strain has an influence on the former. The response of  $E_{cc}$  and  $E_{ee}$  makes  $\mu_{111}$  small in diamond. The charge densities display clearly different response to these strains between diamond and the others since diamond has distinctive two-peak structure of the bond charge and strongly favors the  $sp^3$  hybridization.

In conclusion, the differences of the lattice constants, bulk moduli, and the absolute values of the elastic constants are concerned with the response to the homogeneous volume change, where the kinetic energy plays an important role. The differences of the relative values of the elastic constants, internal strain parameters, and Poisson ratios are closely related to the stability of the  $sp^3$  hybridization, where the ion-electron interaction plays an important role. The distinctive features of diamond can be attributed to the character of a single atom. The most essential point is that the C atom has a smaller volume, that is, a deeper  $p$  pseudopotential than Si and Ge because of the lack of core  $p$  states.

## ACKNOWLEDGMENTS

The author would like to thank A. Koiwai for helpful discussions and informing me of experimental details.

- 
- <sup>1</sup>P. Hohenberg and W. Kohn, Phys. Rev. **136**, B864 (1964); W. Kohn and L. J. Sham, Phys. Rev. **140**, A1133 (1965).  
<sup>2</sup>O. K. Andersen, Phys. Rev. B **12**, 3060 (1975).  
<sup>3</sup>H. L. Skriver, *The LMTO Method. Muffin Tin Orbitals and Electronic Structure* (Springer-Verlag, Berlin, 1984).  
<sup>4</sup>L. H. Weyrich, Phys. Rev. B **37**, 10269 (1988).  
<sup>5</sup>E. Wimmer, H. Krakauer, M. Weinert, and A. J. Freeman, Phys. Rev. B **24**, 864 (1981).  
<sup>6</sup>D. R. Hamann, M. Schlüter, and C. Chiang, Phys. Rev. Lett. **43**, 1494 (1979).  
<sup>7</sup>G. B. Bachelet, H. S. Greenside, G. A. Baraff, and M. Schlüter, Phys. Rev. B **24**, 4745 (1981).  
<sup>8</sup>M. T. Yin and M. L. Cohen, Phys. Rev. B **24**, 6121 (1981).  
<sup>9</sup>B. N. Harmon, W. Weber, and D. R. Hamann, Phys. Rev. B **25**, 1109 (1982).  
<sup>10</sup>M. T. Yin and M. L. Cohen, Phys. Rev. B **26**, 3259 (1982).  
<sup>11</sup>M. T. Yin and M. L. Cohen, Phys. Rev. B **26**, 5668 (1982).  
<sup>12</sup>M. T. Yin and M. L. Cohen, Phys. Rev. Lett. **50**, 2006 (1983).  
<sup>13</sup>J. R. Chelikowsky and S. G. Louie, Phys. Rev. B **29**, 3470 (1984).  
<sup>14</sup>M. T. Yin, Phys. Rev. B **30**, 1773 (1984).  
<sup>15</sup>R. Biswas, R. M. Martin, R. J. Needs, and O. H. Nielsen,

- Phys. Rev. B **30**, 3210 (1984).  
<sup>16</sup>O. H. Nielsen and R. M. Martin, Phys. Rev. B **32**, 3792 (1985).  
<sup>17</sup>P. E. Camp, V. E. Van Doren, and J. T. Devreese, Phys. Rev. B **34**, 1314 (1986).  
<sup>18</sup>O. H. Nielsen, Phys. Rev. B **34**, 5808 (1986).  
<sup>19</sup>G. B. Bachelet, D. R. Hamann, and M. Schlüter, Phys. Rev. B **26**, 4199 (1982).  
<sup>20</sup>E. Wigner, Phys. Rev. **46**, 1002 (1934).  
<sup>21</sup>J. Ihm, A. Zunger, and M. L. Cohen, J. Phys. C **12**, 4409 (1979).  
<sup>22</sup>D. J. Chadi and M. L. Cohen, Phys. Rev. B **8**, 5747 (1973).  
<sup>23</sup>H. J. Monkhorst and J. D. Pack, Phys. Rev. B **13**, 5188 (1976).  
<sup>24</sup>O. H. Nielsen and R. M. Martin, Phys. Rev. Lett. **50**, 697 (1983); Phys. Rev. B **32**, 3780 (1985).  
<sup>25</sup>L. Kleinman, Phys. Rev. **128**, 2614 (1962).  
<sup>26</sup>R. M. Martin, Phys. Rev. B **1**, 4005 (1970).  
<sup>27</sup>M. J. P. Musgrave and J. A. Pople, Proc. R. Soc. London Ser. A **268**, 474 (1962).  
<sup>28</sup>P. N. Keating, Phys. Rev. **145**, 637 (1966).  
<sup>29</sup>J. C. Phillips, *Bonds and Bands in Semiconductors* (Academic, New York, 1973).